Research Square

Preprints are preliminary reports that have not undergone peer review.
They should not be considered conclusive, used to inform clinical practice,
or referenced by the media as validated information.

Neutrophil Extracellular Traps (NETs) drives Blood-Brain Barrier (BBB) leakage, Hippocampal neuronal damage and Cognitive dysfunction: A Therapeutic approach by DNase1

Venkata Sai Konda
GITAM University https://orcid.org/0009-0005-4157-3213
Rahul Kumar.
GITAM University https://orcid.org/0009-0000-1260-3261
Ankit Kumar
GITAM University
Prathyusha koyya
GITAM University
Sri Vidya Ramisetti
GITAM University
Sushmitha Mohan
GITAM University
Rahul Kumar
rkumar2@gitam.edu
GITAM University https://orcid.org/0000-0002-3603-7572

Research Article

Keywords: Cognitive decline, Neutrophil extracellular traps (NETs), Blood Brain Barrier (BBB), inflammation, Hippocampal neuronal damage, neurodegeneration

Posted Date: October 6th, 2026

DOI: https://doi.org/10.21203/rs.3.rs-11265777/v1

License: This work is licensed under a Creative Commons Attribution 4.0 International License. Read Full License

Additional Declarations: The authors declare no competing interests.

Abstract

Cognitive decline represents a critical global health challenge, with cases expected to reach 78 million by 2030. Blood-brain barrier (BBB) disruption has emerged as an early pathological event preceding cognitive impairment, yet the underlying mechanisms remain poorly understood. Neutrophil extracellular traps (NETs) have been implicated in endothelial injury and neurovascular dysfunction, but their specific role in neurodegeneration requires further investigation. This comprehensive study examined the mechanistic contribution of NETs to BBB disruption, neuroinflammation, oxidative stress, mitochondrial dysfunction, and hippocampal neuronal damage using a lipopolysaccharide (LPS)-induced inflammatory mouse model. While DNase1 was administered to degrade NETs and assess therapeutic efficacy. Immunofluorescence studies revealed neutrophil elastase, an abundant component of NETs, accumulated in the hippocampal dentate gyrus and choroid plexus in LPS administered mice. While Behavioral studies performed using Rotarod, Novel Object Recognition (NOR), and Y-maze demonstrated that LPS induced significant deficits in motor coordination, spatial memory, and cognitive function, which were substantially improved by DNase1 treatment. Evans blue dye extravasation assays revealed increased BBB permeability in LPS treated mice, supported by decreased transcript levels of claudin-5 expression. DNase1 administration restored BBB integrity & claudin-5 levels. Biochemical assays revealed that NETs induced oxidative stress and mitochondrial dysfunction, evidenced by altered catalase, superoxide dismutase, lipid peroxidation, and citrate synthase activity, which were ameliorated by DNase1 treatment. qPCR studies confirmed the upregulation of pro-inflammatory cytokines TNF-α, IL-1β, IL-6 in LPS treated mice, which decreased after DNase1 treatment. while H&E staining results showed severe neuronal damage. These findings establish NETs as critical mediators of BBB leakage, an pathological event which precedes neurodegeneration and cognitive decline and identify DNase1 mediated NET clearance as a promising therapeutic strategy for age related cognitive decline.

1. Introduction

Increase in the lifespan due to advancement in the healthcare system had resulted in an increase in the incidence of age associated comorbidities including neurodegenerative, cardiovascular and metabolic diseases. Cognitive impairment is a major health issue for the ageing populations in terms of number, difficulty in detection at early stage, lack of definitive therapy, need for prolonged nursing care and economic cost. There are several vascular anomalies which may play important roles in the pathophysiology of cognitive impairment, including blood brain barrier (BBB) leakage (1, 2), an unique property of brain vasculature by which it tightly regulates the movement of molecules and cells between the brain and blood (3). The major component of the BBB is endothelial cells which are held together with the help of tight junction proteins like claudin, occludin and zona occludens (ZO) (4), which are essential for the maintenance of BBB integrity (5).

BBB impairment can lead to cognitive impairment and neurodegeneration as per several *in vivo* and clinical studies, it is recognized as a major pathological event occurring during the early stages of cognitive impairment (6–9) as well as neurodegenerative diseases like Alzheimer's disease (AD) (10–12). In terms of mechanism, initial compromise in the BBB integrity, creates a potent chemotactic gradient of pro-inflammatory cytokines and chemokines such as IL-1β and TNF- α (19)(20). Activation of brain endothelium by IL-1β and TNF-α upregulate adhesion molecules, facilitating integrin-mediated neutrophil adhesion and subsequent transmigration into the parenchyma (21). Subsequently, neutrophils undergoes a type of cell death termed as NETosis, which was first discovered by Brinkmann *et al* (13) and refers to the release of NETs and involves chromatin de-condensation that occurs through PAD4-mediated deamination of nuclear histones (14). The component of NETs includes cell-free DNA (cfDNA), histones, citrullinated histone H3 (H3Cit), elastase and myeloperoxidase (MPO) (15).

Components of NETs increases with aging as reported by one of our previous studies and others (16–19). We had shown that administration of DNase 1 can reduces the burden of NETs and protect against disease age-related deep vein thrombosis (17). Suttorp *et al* had shown neutrophil elastase can increases the permeability of cultured pulmonary endothelial cell monolayers (20). Furthermore, neutrophil depletion reduces BBB breakdown and increases neovascularization following stroke (21). In addition, depletion of neutrophils using anti-Ly6G can attenuate the severity of AD in transgenic 5xFAD and 3xTg-AD murine models (22). However, at present no studies exists that that systematically evaluate how NETosis mediated BBB disruption during LPS-induced inflammation contributes to cognitive decline. We used LPS-driven murine model of systemic neuroinflammation to understand mechanistic role of NETs mediated cognitive decline and BBB leakage. The mechanistic involvement of NETosis was specifically addressed through intraperitoneal (IP) administration of DNase1, that exhibits the potential to clear NETs through cfDNA degradation. Additionally, the effect of NETosis inhibition was reported on hippocampal and cortical damage, mitochondrial injury, oxidative stress and neuroinflammation.

2. Methodology

2.1 Animals and Treatment plan: We used a total number of 24 animals of 3–4 months old male C57BL/6 mice with average weight of 18–20 grams were procured from the VYAS Labs, Hyderabad, and were quarantined for 5 days for acclimatization in light/dark cycle and ad libitum. The study was approved by the Institutional Animals Ethics Committee (IAEC) and complied with the guidelines set by Committee for the Purpose of Control and Supervision of Experiments on Animal (CPCSEA). Mice were categorized into three different groups with 8 mice in each group as follow: Control (received Saline), LPS (1mg/kg), and DNase1 (1mg/kg). All the treatments were received intraperitoneally followed by weight management throughout the treatment period.
2.2 Immuno-fluorescence study: Immunofluorescence study was performed to visualize the NETs and their components in the Coronal sections of brain(23). Coronal brain sections (5 µm) were fixed in 4% paraformaldehyde, dehydrated through increased concentrations of ethanol, cleared in xylene, and were embedded in paraffin as per the established protocols (24). Heat induced antigen retrieval was performed in 10 mM sodium citrate, pH 6.0 at 95°C, and 0.4% Triton X-100 for 10 minutes was used for permeabilization. Nonspecific binding of endogenous peroxidases was blocked with 3% H_2O_2 in methanol, followed by blocking in 5% BSA. Neutrophils infiltration was probed with rabbit anti-neutrophil elastase IgG (NE; 1:1000) and FITC-conjugated goat anti rabbit IgG (1:5000) from cloud clone corp., was used. Imaging was performed using confocal microscopy from OLYMPUS FUV 4000 and % of area of occupancy in hippocampal dentate gyrus was quantified via ImageJ analysis(25).
2.2 Behavioral Studies:

2.2.1 Rotarod test: The rotarod test is performed for motor coordination and balance in mice(26). The test was conducted for 3 days, which included 2 days of training period and one day for the test. During the training period, each mouse was placed individually on a rod rotating at a constant speed of 10 rpm, where it was allowed to acclimatize and learn to balance its posture. Each mouse underwent three training trials per day (T1, T2, T3), with a 15-minute interval between each trial. Upon completion of each trial, the animals were returned to their home cages for the resting period. On the test day, each mouse was placed on the rotarod apparatus, with the speed of 20 rpm over a 300-second interval. We recorded the elapsed time, which is the latency of each mouse to fall, from the rotarod.
2.2.2 Y Maze test: The Y-maze behavioral study is generally performed to assess the immediate short term memory, The spontaneous alteration behavior of mice is generally recorded to assess the spatial working memory(27). It is conducted using an Y shaped maze-like apparatus composed of three arms positioned symmetrically at 120° angle, with each arm measuring 35 cm in length, 6 cm in width, and 13 cm in height. The procedure initially involved carefully placing mice at center followed by continuously monitoring their different arm entries as exploratory behavior over a fixed 8-minute observation period. Throughout the entire study, a valid arm entry was defined only when the mouse's entire body, including its tail, was fully within an arm, which ensured accuracy in the behavioral assessment. Spontaneous alternations were recorded as consecutive entries into three different arms and percentage of alternation calculated by using the formula below.

$$\varvec{\%\ Of\ Alternation} \Rightarrow \left\{ \frac{\varvec{a}}{} \right.$$

2.2.3 Novel object recognition (NOR) test: NOR assay is usually performed to understand the recognition memory and the spatial working memory in mice(28). The entire study was conducted in an acrylic open field box measuring 40 × 50 × 50 cm, the entire procedure includes three phases: habituation, training, and testing. During the 2-day habituation phase, each mouse was placed individually in the box for 5–10 minutes to acclimate to the environment before being returned to its home cage. During the training period, each mouse was put into the box with two identical objects and given ten minutes to freely explore. After one hour the mice were put back in the test chamber with one familiar object and one new object given ten minutes to explore. Object explorations like rearing and nosing were determined by tracking with the mouse's head near the object with interaction times noted for both familiar and novel objects.

The following formula was used to determine the cognitive index (CI):

$$\varvec{Cognition\ Index}\ (\varvec{}$$

2.3 Assessment of BBB Integrity: 2.3.1. Evans Blue (EB) extravasation test: To analyze the BBB permeability in brain, Mice were administered intraperitoneally with 5 ml/kg of body weight EB followed by euthanization after 4 hours. A part of Brain tissue was homogenized in 50% trichloroacetic acid (w/v) and EB concentration was determined by measuring the absorbance at 610 nm and normalized to the wet weight of brain tissue as described by Manaenko et al (29).
2.3.2 q-PCR for Claudin-5: Total RNA was isolated using TRIzol using the standard procedures and treated with DNase I at 65°C to eliminate genomic DNA contamination. 1 µg of RNA was reverse-transcribed to cDNA using the Revert-Aid First Strand cDNA Synthesis Kit (Invitrogen). Claudin-5 mRNA was amplified using SYBR Green based real-time PCR on a CFX Opus system (Bio-Rad) and expression was quantified using the comparative $2^{-\Delta\Delta CT}$ method, with GAPDH was used as housekeeping reference gene.

All the assays mentioned below were carried out using brain tissue, homogenized in 1.15% KCl prepared in 50 mM phosphate buffer (pH 7.4).
2.4.1 Lipid peroxidation assay: Lipid peroxidation in brain was quantified by measuring malondialdehyde (MDA), using a thiobarbituric acid reactive substances (TBARS) assay(30). Brain tissue homogenate was precipitated by addition of 2.5%(w/v) trichloroacetic acid (TCA) for 5 min, followed by centrifugation at 4,000 rpm for 5 min. The resulting supernatant was mixed with an equal volume of freshly prepared TBA reagent in acetic acid, followed by the incubation at 95°C for 1 hour to allow formation of the MDA–TBA adduct. After cooling to room temperature in a water bath, the absorbance of the pink chromogen was recorded at 532 nm, and MDA concentration was calculated using a molar extinction coefficient of 1.56 × 10^5 $M^{-1}cm^{-1}$. MDA levels were normalized to tissue weight and expressed as nmol/mg of tissue weight.
2.4.2 Catalase Activity: Catalase activity was measured to evaluate the antioxidant defense against hydrogen peroxide (H_2O_2) induced oxidative stress(31). Around 30 µL of tissue homogenate was added to 3 mL of freshly prepared 30 mM H_2O_2 in 50 mM phosphate buffer (PB) (pH-7.0). The changes in the absorbance due to H_2O_2 decomposition was monitored spectrophotometrically at 240 nm for 3 minutes, using a molar extinction coefficient of 43.6 $M^{-1}cm^{-1}$ for H_2O_2 catalase enzyme activity (U/mg) of brain tissue was calculated for enzyme required to decompose 1 µmol of H_2O_2 per minute under the assay conditions.
2.4.3 Superoxide dismutase (SOD) activity: SOD activity in brain tissue was determined by a nitro blue tetrazolium (NBT) reduction assay based on the ability of SOD to inhibit superoxide-driven formazan formation(32). The reaction mixture contained 50 mM sodium carbonate buffer (pH-10.2), 0.1mM EDTA, 1.2 mM NBT, and 1 mM hydroxylamine hydrochloride, to which 50 µl of brain homogenate was added. The increase in absorbance of the NBT formazan complex was monitored spectrophotometrically at 560 nm. SOD activity was calculated from the percentage inhibition of NBT reduction relative to a blank.
2.4.4 Citrate synthase activity: Citrate synthase activity was estimated spectrophotometrically using a optimized protocol from Shepherd et al (33). This assay evaluates the total mitochondrial damage in the brain tissue homogenate. The reaction mixture consists of 50 mM phosphate buffer (pH 7.4), 0.4 mM of 2-nitrobenzoic acid (DTNB), 0.1 mM oxaloacetate, and 0.3 mM acetyl-CoA. The reaction was initiated by adding brain tissue homogenate, and the kinetic changes in absorbance was recorded at 412 nm for 10 minutes using a microplate reader and calculated the specific enzyme activity.

$$\varvec{Specific\ Enzyme\ Activity}\ \varvec{}$$

2.5 Assessment of Pro-/anti neuro inflammatory markers using q-PCR: The transcriptional levels of IL-1β, IL-6, TNF-α, were quantified using Real-Time quantitative PCR (RT-qPCR) with the synthesized cDNA as a template according to section 2.3.2. Amplification was carried out with SYBR Green Master Mix on a CFX Opus Real-Time PCR System (Bio-Rad) with primer sequences listed in Table 1. GAPDH was used as the housekeeping gene, and relative expression was calculated by the $2^{-\Delta\Delta CT}$ method.

2.6 H&E Staining for assessment of Histopathological changes: To observe the changes induced by LPS mediated Inflammation to the cellular architecture and histopathological changes like morphology, cellular damage, pyknotic nuclei, hyperchromatic cells and vacuolation in the mice brain tissue, the brain sections as mentioned in the above section 2.2, after rehydration were stained with hematoxylin for nuclear visualization, and counterstained with eosin to visualize cytoplasmic and extracellular components. Slides were mounted with and observed under microscope followed by Image analysis using FIJI image software and the area covered by the deeply stained neuronal cells, hippocampal cell morphology, Pyknotic nuclei, and vacuolation are quantified using standard Brain Atlas sources and references (34).

2.7 Statistical Analysis

Table 1
shows the forward and reverse Primers sequences used for q-PCR study for pro and anti-inflammatory markers ordered from Eurofins.

Primer sequences used for q-PCR study for pro and Anti inflammatory markers		
Genes	**Forward (5'-3')**	**Reverse (5'-3')**
IL-1β	AGCATCCAGCTTCAAATC	CTTCTCCACAGCCACAAT
IL-6	GACAAAGCCAGAGTCCTTCAGAGAGA	GGTCTTGGTCCTTAGCCACTCCTT
TNF-α	TCTCATTCCTGCTTGTGGC	CACTTGGTGGTTTGCTACG

Oridnary one-way Anova (multiple comparisons) were applied to make statistical comparisons between each groups. The data is represented as mean ± S.E., and any observed statistically significant differences were determined for P values < 0.005. The statistical analyses were performed with GraphPad Prism software (8.0.2).

3. Results

3.1 LPS treatment resulted in the NETs accumulation within Hippocampal Dentate Gyrus, which was cleared using DNase1

In order to determine if DNase1 mediated degradation of cfDNA that can reduces NETs accumulation within the brain parenchyma, we performed immunofluorescence study using rabbit anti NE IgG and FITC conjugated goat anti rabbit IgG. Quantitative analysis of percentage area covered by the NE-FITC signals using ImageJ with adjusted threshold showed a significant increase in NE fluorescence intensity in LPS group versus saline controls ($P < 0.05$) **(**Fig. 1**). Supplementary figure SF1-SF3** shows the NE-FITC signals observed in the dentate gyrus of the hippocampal region at 20x magnifications and **SF4-SF5** represents in higher magnification of 60x. NE signals appeared as granular thread-like structures resembling NETs and predominantly present in the granular cell layers of dentate gyrus, while the regions like Choroid Plexus have shown the direct deposition of these NE signals infiltrating into the Dentate Gyrus. **Supplementary figure S6-SF7.** While DNase1 treatment significantly reduced NE intensity. These results demonstrated that the LPS induced neutrophils infiltration and NETs accumulation within brain parenchyma and, while DNase1 attenuated the neutrophil accumulation and NETs release within dentate gyrus.

3.2 DNase1 mediated NETs clearance mitigated cognitive deficits in mice:

Protective effect of DNase1 mediated NETs clearance on cognitive function and motor coordination was determined using a battery of behavioral tests including rotarod, Y Maze and NOR. Using fix speed rotarod, latency to fall was calculated and we observed a significant decline in the LPS treated group when compared with saline ($P < 0.05$), whereas the animals administered with DNase1 were able to stay on the rotarod for a longer period of time, although the p values were non significant. **(**Fig. 2A**).** Percentage of alterations as determined by Y maze test significantly declines in mice upon treatment with LPS (P), which was mitigated upon DNase1 mediated clearance of NETs **(**Fig. 2B**).** Similarly, mice administered with LPS exhibited a significantly reduced discrimination index (DI) compared to the saline treated mice group as control ($P < 0.05$) using NOR, which implies impaired recognition memory assessed by impaired exploration of a novel object. DNase1 administration following LPS treatment improved the DI ($P > 0.05$), demonstrating the recovery of cognitive function indicated by increased exploration time with novel object **(**Fig. 2C**).** Taken together, these findings suggested that clearance of NETs using DNase1 confers protective effect against NETs dependent cognitive and motor impairment.

3.3 DNase1 attenuates NETs dependent BBB leakage:

We determined the protective effect of NETs inhibition on BBB integrity using EB extravasation and examined the mechanistic involvement of tight junction protein by measuring the transcript level of claudin-5. Quantitative analysis of EB concentrations in the homogenized brain tissues indicated that LPS group exhibited significantly elevated extravasation of EB into the brain parenchyma ($P = 0.01$) compared to saline control, which had minimal EB dye penetration. On the other hand, animals treated with DNase1 exhibited lower penetration of the EB dye into the brain parenchyma **(**Fig. 3A**).**

The quantitative PCR analysis of tight junction protein cluadin-5, indicates decreased transcript levels upon LPS treatment within brain homogenates ($P < 0.05$), which was brought back to the normal upon DNase1 mediated NETs ($p < 0.05$) **(**Fig. 3B**).**

3.4 NETs induce the oxidative stress and mitochondrial damage in brain:

We studied the effect of NETosis on the oxidative stress within brain by measuring the enzymatic activity of catalase, SOD and lipid peroxidation using appropriate biochemical assays. The contribution of mitochondrial impairment was assessed by performing the activity assay for citrate synthase using brain homogenate. The significant increase in NETs dependent ROS accumulation led to structural and functional damage of polyunsaturated fatty acids, generating various reactive aldehydes especially MDA in cell membranes. Elevated levels of MDA when analyzed by TBA based chromogenic assay were found in LPS treated brain tissues indicating increased lipid peroxidation and oxidative stress **(**Fig. 4a**).** While DNase1 treated mice subsequently lowered MDA levels ($P < 0.05$) almost equal to saline controls, to possibly restore the cell membrane integrity and reducing NETs mediated oxidative damage.

LPS administration in the mice brain resulted in noticeable reduction in catalase activity within brain homogenate when compared to control ($P < 0.05$). This decrease in catalase activity reflects the inability of neural tissue to efficiently reduce the exogenous H_2O_2. We also observed that DNase1 treatment, restored catalase activity ($P < 0.05$) to the level of control group, indicating DNase1 ameliorates NETs-mediated oxidative damage **(**Fig. 4b**).** To our surprise, we could not find any noticeable difference among different groups in terms of SOD activity **(**Fig. 4c**)**, thus ruling out the possibility of free oxygen radicals in mediating NETs dependent oxidative damage, which was primarily driven through peroxide dependent mechanisms.

We found a considerable reduction in specific enzyme activity of citrate synthase in the LPS treated brain homogenates when compared to control groups. Additionally, brain homogenates from the animals treated with DNase1 exhibited pattern of increased citrate synthase activity comparatively similar to the saline group **(**Fig. 4d**).** Although data indicated that NETs accumulation within brain is responsible for the compromised mitochondrial function as indicated by the activity assay for citrate synthase, the values did not reach statistical significance.

3.5 NETs accumulation resulted in the elevation of pro-inflammatory cytokines

qPCR analysis demonstrated that NETs dependent elevation in the level of pro-inflammatory cytokines like IL-6, TNF-α, and IL-1β was reversed upon Dnase1 mediated NETs degradation (Fig. 5A-D**).** This suggests that LPS induced neuroinflammatory response via NET formation amplified the inflammatory signaling responsible for the increased levels of pro inflammatory cytokines like IL6, TNF-α, and IL-1β within the brain tissue, that facilitates further neutrophils and other immune cells recruitment contributing to neuronal injury.

3.6 Histopathological studies reveal hippocampal neuronal injury:

The coronal sections of brain stained with H&E when analyzed for the area covered by the deeply stained neurons using Fiji software, we found that the LPS-treated mice brain exhibited higher infiltration of inflammatory cells **(**Fig. 6**).** The hippocampal cell layers appeared less compact and more diffused than usual organized arrangement of neuronal cells within the Dentate gyrus regions of brain sections collected from LPS treated mice when compared with control group. In addition, several cells displayed the intense dark blue stained nuclei, with condensed and shrunken appearance suggesting hyperchromatic or pyknotic morphology in higher magnifications (**Supplementary figure SF8-9)**. DNase1 treated mice brain exhibited similar dark blue stained, condensed pyknotic nuclear arrangement in Dentate Gyrus while lesser inflammatory cells were noted indicating possible NET clearance.

4. Discussion

In our present study we elucidated the mechanistic role of NETs in BBB leakage which precedes the age associated comorbidities like cognitive decline using LPS induced inflammatory model which has been widely accepted to induce NETs release (38). One of our previous studies reported an elevation in the circulating markers for NETs in aged population and thus indicates their potential involvement in various age-related comorbidities, including cognitive impairment (17). The current study described the mechanistic involvement of NETs in cognitive impairment modelled using LPS treatment in mice.

Our major findings include that the LPS treated mice have shown the direct deposition of the NE, an abundant protein released by neutrophils, signals within the hippocampal, dentate gyrus, choroid plexus regions. LPS induced NETs release reduced the expression levels of claudin-5, an abundant endothelial tight junction protein, that corroborates with the increased BBB leakage as examined using EB extravasation. This is further supported by significant motor & cognitive deficits characterized by increased latency to fall in the rotarod test, decreased percentage of alterations in the Y-maze, and reduced discrimination index in the NOR test, while DNase1 treatment mitigated the effects. We further observed the presence of deeply stained neuronal cells, severe vacuolation, nuclear pyknosis, and reduced cellular density, across the dentate gyrus, using H&E staining, which directly explains the spatial and recognition memory deficits observed in our behavioral studies. The results obtained were in line with the previous studies reports indicating the involvement of neutrophils activation in the AD using transgenic 5xFAD and 3xTg-AD models (22) and also in Traumatic Brain Injury where the neutrophils actively infiltrated through Choroid plexus region into CSF and vascular tissues in brain (35, 36).

To elucidate the cellular mechanism driving these behavioral deficits, we further identified that the LPS induced NETs upregulates pro-inflammatory cytokines and resulted in excessive production of ROS. This oxidative stress overwhelmed cellular antioxidant defenses evidenced by decreased catalase activity while elevating lipid peroxidation and impaired mitochondrial function. In contrast, DNase1 mediated clearance of NETs rescued the mice from these effects, revealing informative biological patterns despite some variance in statistical significance. NETs and their enzymes damage the endothelial cells of BBB facilitating the further recruitment of peripheral immune cells which creates a vicious cycle of cytokines and other immune cells promoting further neutrophil infiltration, which in turn increases the BBB permeability (37, 38). The inflammatory cellular load and histopathological features are consistent with previous studies where NETs-driven toll like receptor 9 (TLR9) activation induced neuronal endoplasmic reticulum (ER) stress and apoptosis, a mechanism recently found to be implicated in the traumatic brain injury and likely operative in LPS-driven neuroinflammation as well (39, 40).

An FDA-approved DNase1 formulation termed Pulmozyme (dornase alfa) is a prescription inhaled enzyme used alongside standard therapies for the management of cystic fibrosis (41). Since the formulation is already FDA approved, the initiation of clinical trials will not require prolonged studies for examining toxicity and safety. While there are PAD4 inhibitors like GSK-484 and THIQs that suppress NET formations, they require optimizations and micromolar concentrations make them unsuitable for clinical development which leaves critical gap for therapeutics to clear NET burden (42, 43). Hence, DNase1 dependent clearance of NETs holds the potential as a novel therapeutic approach for the disorders based on NETs release and accumulation.

In summary, clearance of NETs through DNase1 administration mitigated LPS-induced cognitive dysfunction and its associated pathological hallmarks, including BBB disruption, oxidative stress, neuroinflammation, and neurodegeneration. These findings can be further explored in diverse experimental models such as age-related cognitive decline and transgenic models of neurodegenerative diseases. Moreover, this work establishes a foundation for future clinical trials aimed at evaluating the therapeutic potential of DNase1-mediated NETs clearance in the context of neurodegenerative disorders.

Declarations

Acknowledgements:

The authors gratefully acknowledge the MURTI SEIF-CLSM facility provided through the DST-PURSE Grant SR/PURSE/2023/169(G) and MURTI GRIG Funds for funding the research study.

References

1. Zipser BD, Johanson CE, Gonzalez L, Berzin TM, Tavares R, Hulette CM et al (2007) Microvascular injury and blood-brain barrier leakage in Alzheimer's disease. Neurobiol Aging 28(7):977–986. 10.1016/j.neurobiolaging.2006.05.016 PubMed PMID: 16782234
2. Erickson MA, Banks WA (2013) Blood-brain barrier dysfunction as a cause and consequence of Alzheimer's disease. J Cereb Blood Flow Metab 33(10):1500–1513. 10.1038/jcbfm.2013.135 PubMed PMID: 23921899; PubMed Central PMCID: PMC3790938
3. Villabona-Rueda A, Erice C, Pardo CA, Stins MF (2019) The Evolving Concept of the Blood Brain Barrier (BBB): From a Single Static Barrier to a Heterogeneous and Dynamic Relay Center. Front Cell Neurosci 13:405. 10.3389/fncel.2019.00405 PubMed PMID: 31616251; PubMed Central PMCID: PMC6763697
4. Sweeney MD, Sagare AP, Zlokovic BV (2018) Blood–brain barrier breakdown in Alzheimer disease and other neurodegenerative disorders. Nat Rev Neurol 14(3):3. 10.1038/nrneurol.2017.188
5. Nitta T, Hata M, Gotoh S, Seo Y, Sasaki H, Hashimoto N et al (2003) Size-selective loosening of the blood-brain barrier in claudin-5–deficient mice. J Cell Biol 161(3):653–660. 10.1083/jcb.200302070 PubMed PMID: 12743111; PubMed Central PMCID: PMC2172943
6. Montagne A, Barnes SR, Sweeney MD, Halliday MR, Sagare AP, Zhao Z et al (2015) Blood-brain barrier breakdown in the aging human hippocampus. Neuron 85(2):296–302. 10.1016/j.neuron.2014.12.032 PubMed PMID: 25611508; PubMed Central PMCID: PMC4350773
7. Blennow K, Wallin A, Fredman P, Karlsson I, Gottfries CG, Svennerholm L (1990) Blood-brain barrier disturbance in patients with Alzheimer's disease is related to vascular factors. Acta Neurol Scand 81(4):323–326. 10.1111/j.1600-0404.1990.tb01563x PubMed PMID: 2360400
8. Bowman GL, Kaye JA, Quinn JF (2012) Dyslipidemia and blood-brain barrier integrity in Alzheimer's disease. Curr Gerontol Geriatr Res 2012:184042. 10.1155/2012/184042 PubMed PMID: 22654903; PubMed Central PMCID: PMC3359662
9. Hultman K, Strickland S, Norris EH (2013) The APOE ε4/ε4 genotype potentiates vascular fibrin(ogen) deposition in amyloid-laden vessels in the brains of Alzheimer's disease patients. J Cereb Blood Flow Metab 33(8):1251–1258. 10.1038/jcbfm.2013.76 PubMed PMID: 23652625; PubMed Central PMCID: PMC3734776
10. Chai AB, Leung GKF, Callaghan R, Gelissen IC (2020) P-glycoprotein: a role in the export of amyloid-β in Alzheimer's disease? FEBS J 287(4):612–625. 10.1111/febs.15148 PubMed PMID: 31750987
11. Chiu C, Miller MC, Monahan R, Osgood DP, Stopa EG, Silverberg GD (2015) P-glycoprotein expression and amyloid accumulation in human aging and Alzheimer's disease: preliminary observations. Neurobiol Aging 36(9):2475–2482. 10.1016/j.neurobiolaging.2015.05.020 PubMed PMID: 26159621
12. Cirrito JR, Deane R, Fagan AM, Spinner ML, Parsadanian M, Finn MB et al (2005) P-glycoprotein deficiency at the blood-brain barrier increases amyloid-beta deposition in an Alzheimer disease mouse model. J Clin Invest 115(11):3285–3290 25247 PubMed PMID: 16239972; PubMed Central PMCID: PMC1257538
13. Brinkmann V, Reichard U, Goosmann C, Fauler B, Uhlemann Y, Weiss DS et al (2004) Neutrophil Extracell Traps Kill Bacteria Sci 303(5663):1532–1535. 10.1126/science.1092385
14. Wang Y, Li M, Stadler S, Correll S, Li P, Wang D et al (2009) Histone hypercitrullination mediates chromatin decondensation and neutrophil extracellular trap formation. J Cell Biol 184(2):205–213. 10.1083/jcb.200806072 PubMed PMID: 19153223; PubMed Central PMCID: PMC2654299
15. de Bont CM, Boelens WC, Pruijn GJM (2019) NETosis, complement, and coagulation: a triangular relationship. Cell Mol Immunol 16(1):19–27. 10.1038/s41423-018-0024-0 PubMed PMID: 29572545; PubMed Central PMCID: PMC6318284
16. Martinod K, Witsch T, Erpenbeck L, Savchenko A, Hayashi H, Cherpokova D et al (2017) Peptidylarginine deiminase 4 promotes age-related organ fibrosis. J Exp Med 214(2):439–458. 10.1084/jem.20160530 PubMed PMID: 28031479; PubMed Central PMCID: PMC5294849
17. Kumar R, Sonkar VK, Swamy J, Ahmed A, Sharathkumar AA, Pierce GL et al (2022) DNase 1 Protects From Increased Thrombin Generation and Venous Thrombosis During Aging: Cross-Sectional Study in Mice and Humans. J Am Heart Assoc 11(2):e021188. 10.1161/JAHA.121.021188 PubMed PMID: 35023342; PubMed Central PMCID: PMC9238525

18. Matsuda Y, Itabashi M, Tachibana Y, Sugihara T, Sakashita Y, Matsubara T et al (2019) Citrullinated histone H3 expression in anti-neutrophil cytoplasmic antibody-associated vasculitis in older Japanese autopsy patients. Geriatr Gerontol Int 19(3):259–264. 10.1111/ggi.13596 PubMed PMID: 30623538
19. Jylhävä J, Nevalainen T, Marttila S, Jylhä M, Hervonen A, Hurme M (2013) Characterization of the role of distinct plasma cell-free DNA species in age-associated inflammation and frailty. Aging Cell 12(3):388–397. 10.1111/acel.12058 PubMed PMID: 23438186
20. Suttorp N, Nolte A, Wilke A, Drenckhahn D (1993) Human neutrophil elastase increases permeability of cultured pulmonary endothelial cell monolayers. Int J Microcirc Clin Exp 13(3):187–203 PubMed PMID: 8125708
21. Kang L, Yu H, Yang X, Zhu Y, Bai X, Wang R et al (2020) Neutrophil extracellular traps released by neutrophils impair revascularization and vascular remodeling after stroke. Nat Commun 11(1):1. 10.1038/s41467-020-16191-y
22. Zenaro E, Pietronigro E, Della Bianca V, Piacentino G, Marongiu L, Budui S et al (2015) Neutrophils promote Alzheimer's disease-like pathology and cognitive decline via LFA-1 integrin. Nat Med 21(8):880–886. 10.1038/nm.3913 PubMed PMID: 26214837
23. Abu Abed U, Brinkmann V (2019) Immunofluorescence Labelling of Human and Murine Neutrophil Extracellular Traps in Paraffin-Embedded Tissue. JoVE 15160115. 10.3791/60115
24. Park JJ, Cunningham MG (2007) Thin Sectioning of Slice Preparations for Immunohistochemistry. JoVE 3194. 10.3791/194
25. Schneider CA, Rasband WS, Eliceiri KW (2012) NIH Image to ImageJ: 25 years of image analysis. Nat Methods 9(7):671–675. 10.1038/nmeth.2089
26. Dunham NW, Miya TS (1957) A Note on a Simple Apparatus for Detecting Neurological Deficit in Rats and Mice**College of Pharmacy, University of Nebraska, Lincoln 8. J Am Pharm Association (Scientific ed) 46(3):208–209. 10.1002/jps.3030460322
27. Kraeuter AK, Guest PC, Sarnyai Z (2019) The Y-Maze for Assessment of Spatial Working and Reference Memory in Mice. In: Guest PC, editor. Pre-Clinical Models [Internet]. New York, NY: Springer New York; [cited 2026 Sep 28]. pp. 105–11. (Methods in Molecular Biology). Available from: http://link.springer.com/10.1007/978-1-4939-8994-2_10 doi:10.1007/978-1-4939-8994-2_10
28. Ennaceur A, Delacour J (1988) A new one-trial test for neurobiological studies of memory in rats. 1: Behavioral data. Behav Brain Res 31(1):47–59. 10.1016/0166-4328(88)90157-X
29. Manaenko A, Chen H, Kammer J, Zhang JH, Tang J (2011) Comparison Evans Blue injection routes: Intravenous versus intraperitoneal, for measurement of blood–brain barrier in a mice hemorrhage model. J Neurosci Methods 195(2):206–210. 10.1016/j.jneumeth.2010.12.013
30. Ohkawa H, Ohishi N, Yagi K (1979) Assay for lipid peroxides in animal tissues by thiobarbituric acid reaction. Anal Biochem 95(2):351–358. 10.1016/0003-2697(79)90738-3
31. Beers RF, Sizer IW (1952) A spectrophotometric method for measuring the breakdown of hydrogen peroxide by catalase. J Biol Chem 195(1):133–140 PubMed PMID: 14938361
32. Weydert CJ, Cullen JJ (2010) Measurement of superoxide dismutase, catalase and glutathione peroxidase in cultured cells and tissue. Nat Protoc 5(1):51–66. 10.1038/nprot.2009.197
33. Shepherd D, Garland PB (1969) The kinetic properties of citrate synthase from rat liver mitochondria. Biochem J 114(3):597–610. 10.1042/bj1140597
34. Schindelin J, Arganda-Carreras I, Frise E, Kaynig V, Longair M, Pietzsch T et al (2012) Fiji: an open-source platform for biological-image analysis. Nat Methods 9(7):676–682. 10.1038/nmeth.2019
35. Szmydynger-Chodobska J, Strazielle N, Zink BJ, Ghersi-Egea JF, Chodobski A (2009) The Role of the Choroid Plexus in Neutrophil Invasion after Traumatic Brain Injury. J Cereb Blood Flow Metab 29(9):1503–1516. 10.1038/jcbfm.2009.71
36. Marques F, Sousa JC (2015) The choroid plexus is modulated by various peripheral stimuli: implications to diseases of the central nervous system. Front Cell Neurosci 9. 10.3389/fncel.2015.00136
37. Cruz Hernández JC, Bracko O, Kersbergen CJ, Muse V, Haft-Javaherian M, Berg M et al (2019) Neutrophil adhesion in brain capillaries reduces cortical blood flow and impairs memory function in Alzheimer's disease mouse models. Nat Neurosci 22(3):413–420. 10.1038/s41593-018-0329-4
38. Santos-Lima B, Pietronigro EC, Terrabuio E, Zenaro E, Constantin G (2022) The role of neutrophils in the dysfunction of central nervous system barriers. Front Aging Neurosci 14:965169. 10.3389/fnagi.2022.965169
39. Jin J, Wang F, Tian J, Zhao X, Dong J, Wang N et al (2023) Neutrophil extracellular traps contribute to coagulopathy after traumatic brain injury. JCI Insight 8(6):e141110. 10.1172/jci.insight.141110
40. Scholz M, Cinatl J, Schädel-Höpfner M, Windolf J (2007) Neutrophils and the blood–brain barrier dysfunction after trauma. Med Res Rev 27(3):401–416. 10.1002/med.20064
41. Terlizzi V, Castellani C, Taccetti G, Ferrari B (2022) Dornase alfa in Cystic Fibrosis: indications, comparative studies and effects on lung clearance index. Ital J Pediatr 48:141. 10.1186/s13052-022-01331-5 PubMed PMID: 35927765; PubMed Central PMCID: PMC9351191
42. Martinez NE, Zimmermann TJ, Goosmann C, Alexander T, Hedberg C, Ziegler S et al (2017) Tetrahydroisoquinolines: New Inhibitors of Neutrophil Extracellular Trap (NET) Formation. ChemBioChem 18(10):888–893. 10.1002/cbic.201600650
43. Lewis HD, Liddle J, Coote JE, Atkinson SJ, Barker MD, Bax BD et al (2015) Inhibition of PAD4 activity is sufficient to disrupt mouse and human NET formation. Nat Chem Biol 11(3):189–191. 10.1038/nchembio.1735

Figures

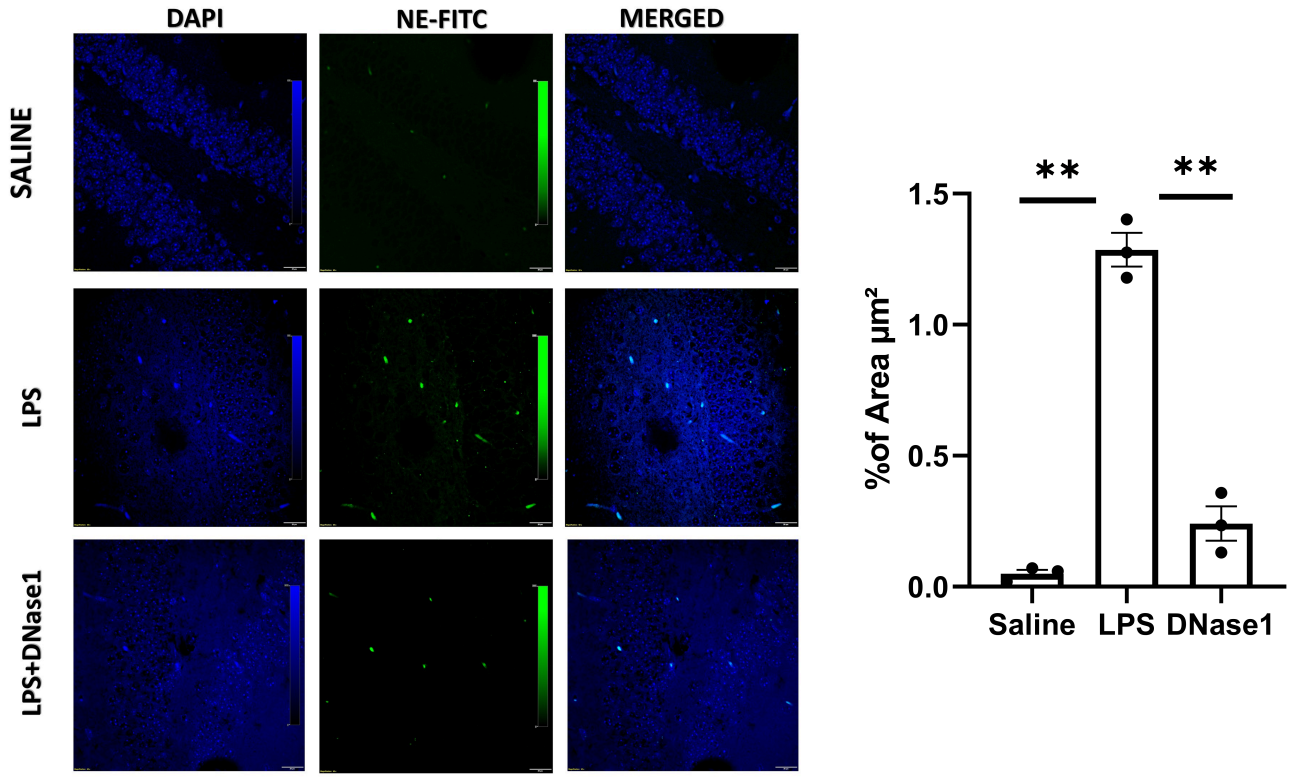


Figure 1

DNase I treatment significantly clears neutrophil extracellular traps (NETs) deposited in the hippocampal dentate gyrus.

LPS treatment induces neutrophil recruitment, upon activation they release NETs, web-like chromatin structures along with proteases such as neutrophil elastase (NE). Following LPS induced BBB leakage, these NETs infiltrate and accumulate within the granular cells of dentate gyrus of the hippocampus. The figure represents immunofluorescence study with corresponding quantification of NE expression (FITC, green) using ImageJ (1.54g) acquired at 60× magnification, which also demonstrates the effect of DNase I in degrading localized NET deposition. *{N= 3, Mean ± SE, One way Anova, **P < 0.05}*

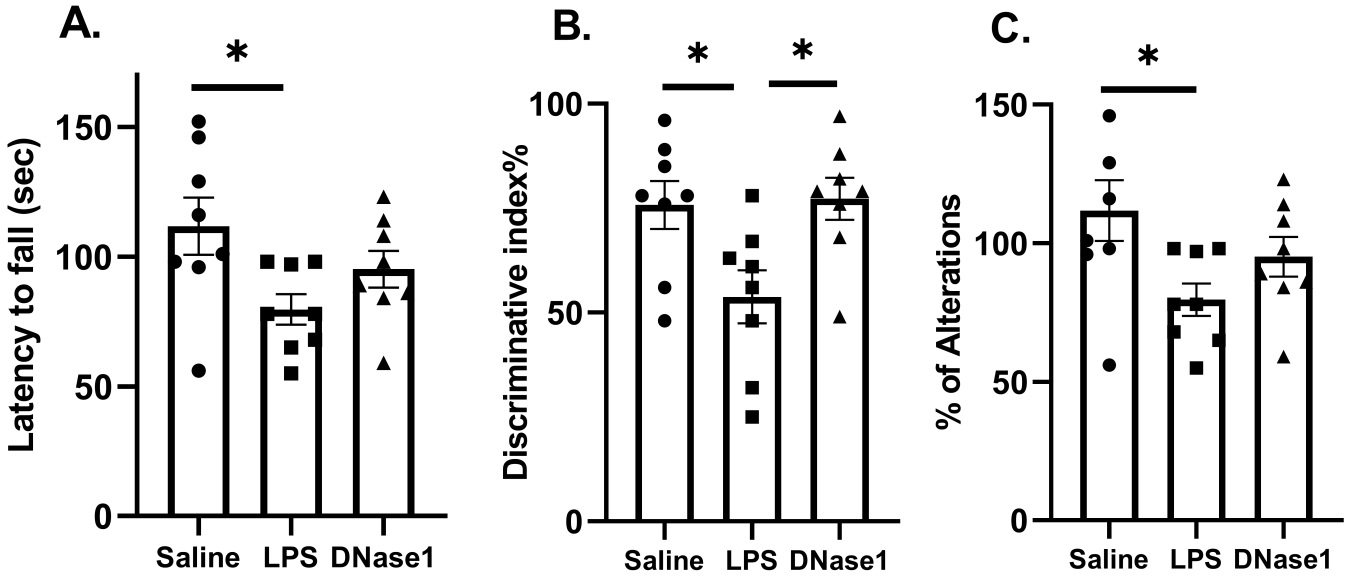


Figure 2

DNase1 treatment improved the LPS-induced NETosis mediated motor and cognitive dysfunction revealed by A. Rotarod, B. Novel Object Recognition(NOR), C. Y-maze Assay.

Systemic LPS administration induced NETs release, compromised BBB integrity leading to neuroinflammation. This resulted in significant motor and Cognitive impairments. The above figure represents (A) The Rotarod assay demonstrates compromised motor grip strength, coordination and balance as seen in latency to fall increased in LPS treated mice (B) NOR assay reveals significant deficits in non-spatial recognition memory explained by reduced discrimination between objects. (C) The Y-maze assay highlights reduced spontaneous alternation, indicating compromised spatial working memory in LPS treated mice. Whereas DNase1 treated mice have shown improved latency to fall, reduced discriminative index and improved alteration percentage suggests Successful clearance of NETs restored BBB repair and lead to improve the cognitive function. All behavioral assays were performed in same environment. *{N= 8, Mean ± SE, One way Anova, *P <0.05}*

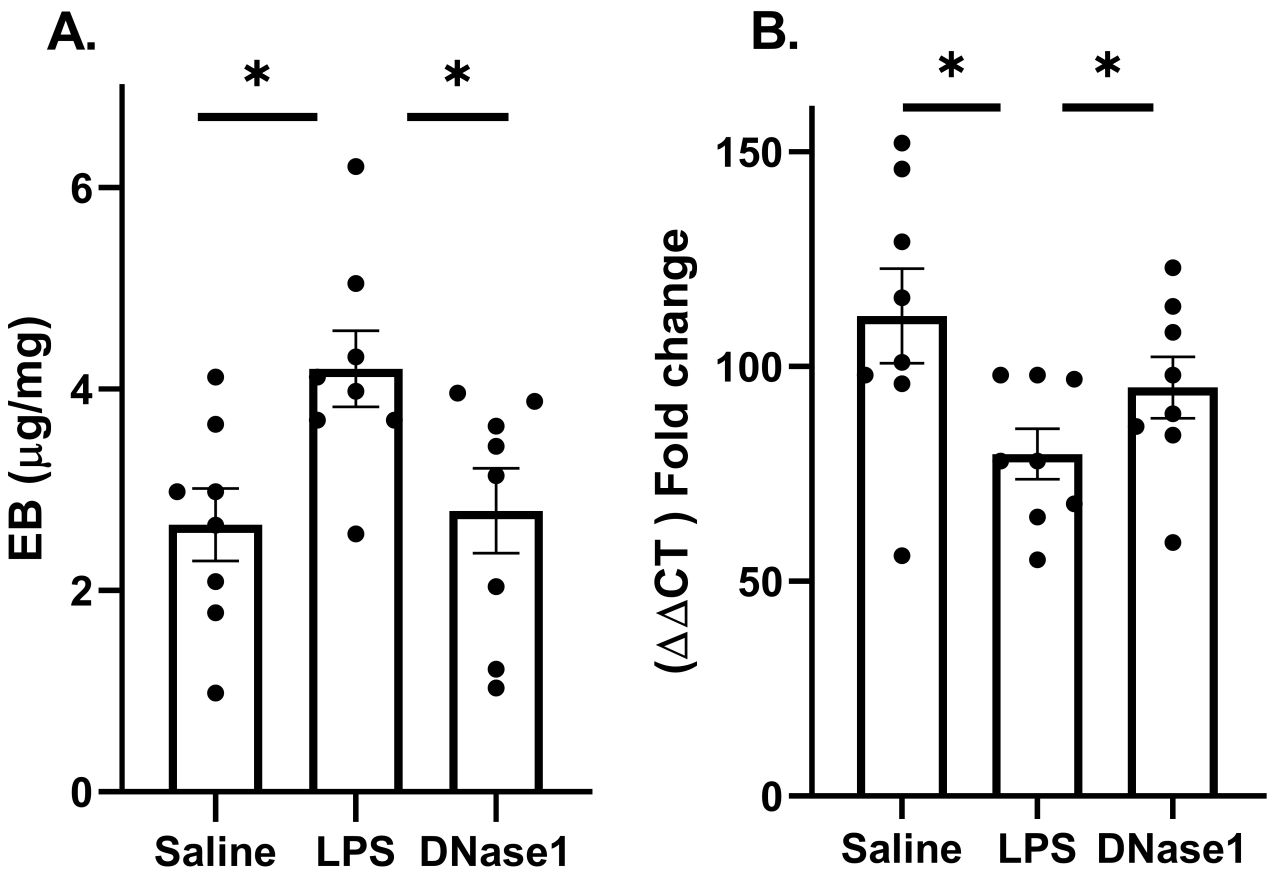


Figure 3

LPS induced NETs release disrupts BBB integrity, represented by increased A) Evans blue extravasation and altered B) Claudin-5 expression. Quantification of BBB leakage, represented by increased **A)** Evans blue dye extravasation was measured spectrophotometrically in brain tissue homogenates (absorbance at 620 nm). **(B)** Alteration of Claudin-5 expression represented by relative mRNA transcript levels estimated via SYBR Green-based qPCR using $2^{-\Delta\Delta CT}$ method and normalized to a stable GAPDH housekeeping gene *{N= 8, Mean ± SE, One way Anova, *P <0.05}.*

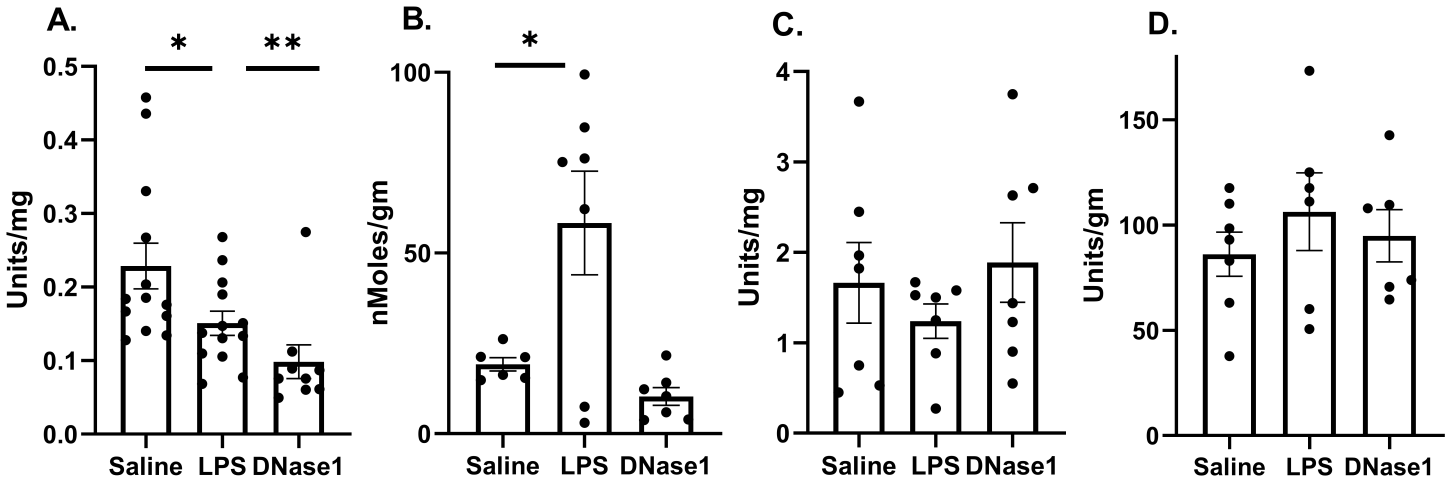


Figure 4

LPS-induced NETs mediated oxidative stress and mitochondrial dysfunction are reflected by changes in A. lipid peroxidation B. catalase, C. SOD, and D. Citrate synthase activity.

*The NET mediated ROS production overwhelms the antioxidant defenses and thus damages the cell membrane and mitochondrial activity. The figure represents the membrane damage by A) Lipid peroxidation and compromised antioxidant defenses such as B) Catalase C) SOD and mitochondrial damage by d) Citrate synthase estimated spectrophotometrically {N= 8, Mean ± SE, One way Anova, *P <0.05}.*

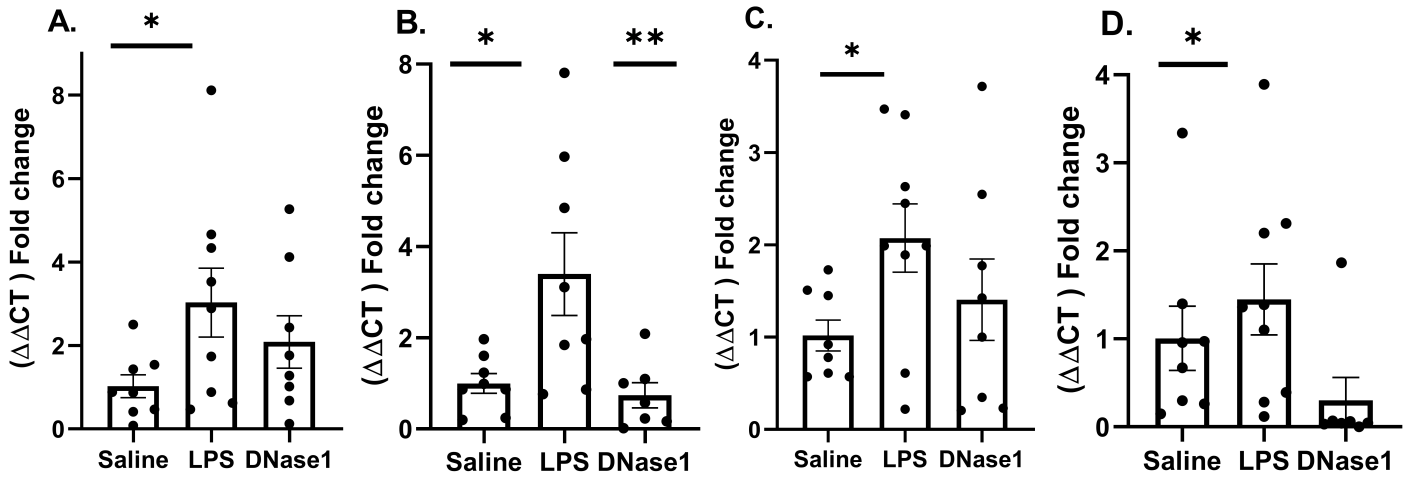


Figure 5

Systemic LPS challenge triggers increased release of pro-inflammatory cytokines from resident brain cells like a) IL-6, b) TNF-α, c) IL1βwhich creates chemotrophic signaling essential for neutrophil activation and recruitment mediating further neuroinflammation. The elevated levels of the above mentioned pro inflammatory cytokines were quantified with the q-PCR SYBR Green assay using their mRNA transcripts from RNA synthesis and CDNA preparation by $2^{-\Delta\Delta CT}$ method and the fold change values are normalized to GAPDH. *{N= 8, Mean ± SE, One way Anova, *P <0.05}*

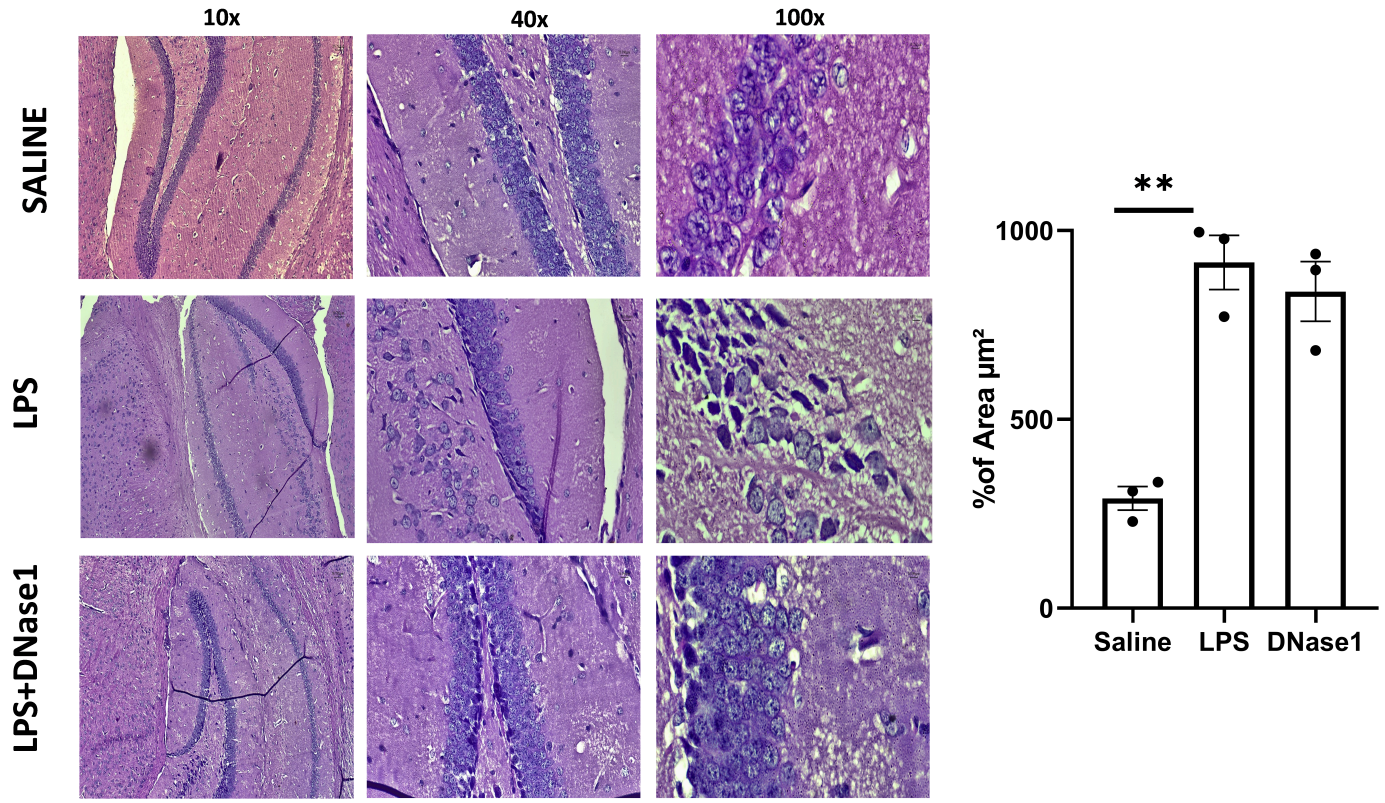


Figure 6

H&E Staining studies represents LPS treated mice brain sections shown hyperchromatic cells with pyknotic morphology and diffused cellular arrangement in Hippocampal Dentate gyrus region compared to saline. Photomicrographs were taken using Light microscope at 10x,40x and 100x and were quantified by measuring the % of area occupied by the hyperchromatic cells, deconvoluting the images using FIJI software, *{N= 3, Mean ± SE, One way Anova, ***P <0.05}*.

Supplementary Files

This is a list of supplementary files associated with this preprint. Click to download.

- ABSTRACTIMAGEOFTHEENTIRESTUDY.png